MICS JOURNAL

Mathematics-in-Industry Case Studies Journal, Volume 4, pp. 1-13 (2012)

A variational approach to modeling aircraft hoses and flexible conduits

Ke Han [*] Huiyi Hu [†] Eunkyung Ko [‡] Ahmet Ozkan Ozer [§] Cory Simon [¶]
Changhui Tan [‖]

Abstract. Airplanes have thousands of hoses and flexible conduits in conjunction with moving parts, and it is essential that the conduits do not tangle or kink and that the minimal amount of material is used to minimize weight. To prevent the necessity of building plywood prototypes and arranging hoses by trial and error, the simulation of the resting states of the conduits serves as a tool for design. Here, we model the resting state of a conduit as being a critical point of the elastic energy functional– the integral of the square curvature– in neglecting gravity, torsion, and shape memory. Using a variational approach, we find the Euler-Lagrange equations for the critical point of the energy functional. We use a robust, parametric representation for the centerline of the conduit in three dimensional space and consider both free length and constrained length problems using the Lagrangian multiplier method. The ultimate goal towards which we step with this work is to, with a bottoms-up approach, use large-scale simulations in the design of the positions and slopes of the fittings of and lengths of conduits used in aircraft construction. This problem was brought by The Boeing Company to a student modeling camp at the Institute for Mathematics and its Applications in 2011, and this paper describes the solution found by the student team.

Keywords. elastic energy functional, modeling flexible hoses, minimizing curvature, Euler-Lagrange equations

1 Introduction

Hoses and flexible conduits are ubiquitous (e.g., garden hoses, laptop power chords, Figure 1 (a)). In the context of an aircraft, thousands of flexible conduits are used in the construction to encapsulate electrical wires, fluids, etc. and are often in conjunction with moving parts (see Figure 1

[*]Pennsylvania State University han@math.psu.edu
[†]University of California, Los Angeles huiyihu@math.ucla.edu
[‡]Mississippi State University ek94@msstate.edu
[§]University of Waterloo aozer@uwaterloo.ca
[¶]University of British Columbia [corresponding author] CoryMSimon@gmail.com
[‖]University of Maryland jefftan@math.umd.edu

(b)). A desirable design prevents any interactions that induce stresses in the conduits that can cause material damage and uses the minimal amount of material necessary. Before simulations were viable, The Boeing Company built prototype airplanes made of plywood, drilled holes, and attempted to optimally arrange the necessary tubing through trial and error. Simulating the configurations of the conduits would enable The Boeing Company to arrange the myriad of conduits *without* building a time-consuming, expensive plywood prototype of the aircraft. The focus of this work is to model the resting shape of a single flexible conduit, which is a step towards large-scale simulation.

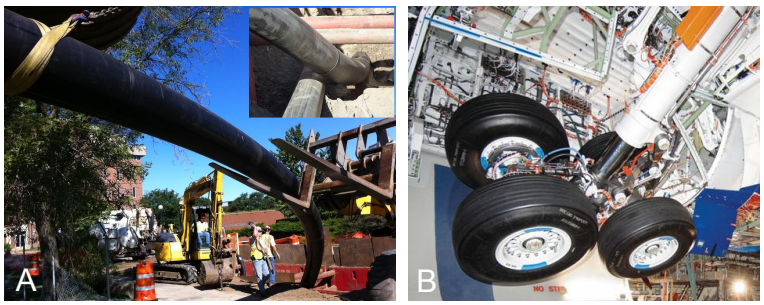

Figure 1: *(a) A giant conduit for transporting chilled water at a construction zone. (b) Hundreds of flexible conduits in the landing gear of an airplane. Each of these conduits changes shape as the landing gear retracts.*

We are concerned with hoses and conduits, much like garden hoses, that are attached by means of fittings that enable torsion-free movement at the ends. Our goal is to determine the equilibrium shape that a flexible conduit will take given the position and angles of the fittings. A flexible hose or conduit can be modeled as a spring; when it is bent into a nonlinear shape, an internal stress is induced by the compression and stretching of the material below and above, respectively, the center line of the conduit. Bernoulli purposed a simple model for the energy a curve stores when it takes a particular orientation in space by summing up the internal stresses at each point [1], modeling the energy of an elastic curve as proportional to:

$$J = \int_{s_0}^{s_1} \kappa^2(s) ds, \tag{1}$$

where the curvature κ is a function of the arc length s of the curve parameterized from s_0 to s_1. The above formulation neglects any effects of gravity, shape memory, or torsion. Given the orientation of its fittings and any length constraints, each conduit will naturally be in a configuration that minimizes its potential energy given by J. We find the critical point (a function) of the potential energy functional (1) for a bent conduit to find the equilibrium shape when the ends of the conduit are attached at prescribed positions and angles. Our mathematical approach for minimizing the functional J is the calculus of variations, an extension of calculus that treats the problem of

minimizing an integral over a space of functions.

In this work, we use a robust, parametric representation of a curve that models the centerline of the conduit and also consider a less robust, but simpler, representation that reduces computational costs. Using the calculus of variations and the Lagrangian multiplier method, we find the Euler-Lagrange equations that describe the shape that the conduit will take in its resting state. Finally, we provide some sample simulations for illustration, where we numerically solve the resulting fourth-order Euler-Lagrange differential equations using a collocation method.

2 Modeling the equilibrium shape of a conduit

We model the centerline of the conduit with a curve in 3-dimensional space parameterized by s; $\mathbf{y}(s) : [0,1] \to \mathbb{R}^3$ and assume the curve is in $C^4([0,1])$. The curvature κ of the curve at a point s is defined to be $\kappa(s) = 1/R(s)$, where $R(s)$ is the radius of the circle which best-approximates the curve at the point $\mathbf{y}(s)$. The unsigned curvature

$$\kappa(s) = \frac{\|\mathbf{y}' \times \mathbf{y}''\|}{\|\mathbf{y}'\|^3}.$$

If the parameterization is chosen such that $\|\mathbf{y}'(s)\|$ is a constant (i.e. constant speed parametrization), then $\kappa(s)$ is proportional to $\|\mathbf{y}''(s)\|$. In this constant speed parameterization scenario, the total potential energy is proportional to

$$J(\mathbf{y}) = \int_0^1 \mathbf{y}'' \cdot \mathbf{y}'' \, ds. \tag{2}$$

Our objective is to minimize J among all functions $\mathbf{y}$ which satisfy proper boundary conditions in order to find the resting state of the conduit. We consider both free length and constrained length problems, and in both we consider the boundary conditions $\mathbf{y}(\mathbf{0}) = \mathbf{y_0}$, $\mathbf{y}(\mathbf{1}) = \mathbf{y_1}$, $\mathbf{y}'(\mathbf{0}) = \mathbf{v_0}$, $\mathbf{y}'(\mathbf{1}) = \mathbf{v_1}$ that correspond to the two endpoints of the conduit attached to fittings at specified positions and slopes.

2.1 The free length problem

First, we consider the case when the total length of the curve $\mathbf{y}(s)$ is unrestricted. So that the potential energy is expressed by J in (2), we induced the constraint of constant speed parameterization. Differentiating $\|\mathbf{y}'(s)\| =$ constant, we have $\mathbf{y}'(s) \cdot \mathbf{y}''(s) = 0$ for all $s \in [0,1]$. Note that $\int_0^1 (\mathbf{y}' \cdot \mathbf{y}'')^2 ds = 0$ implies $\mathbf{y}'(s) \cdot \mathbf{y}''(s) = 0$ for all $s \in [0,1]$, which imposes the constant parameterization speed. We minimize J among all curves $\mathbf{y}(s) \in C^4([0,1])$ that satisfy proper boundary conditions and $\int_0^1 (\mathbf{y}' \cdot \mathbf{y}'')^2 ds = 0$, and this gives the minimal energy configuration of the conduit under no length constraint. Using the Lagrangian multiplier method [8], we obtain the energy minimization problem:

$$\text{Minimize } J_\lambda(\mathbf{y}) = \int_0^1 \left(\mathbf{y}'' \cdot \mathbf{y}'' + \lambda \, (\mathbf{y}' \cdot \mathbf{y}'')^2\right) ds. \tag{3}$$

With the constant parameterization speed constraint expressed with this integral form, the parameter λ is a scalar.

Let $f(\mathbf{y}, \mathbf{y}', \mathbf{y}'') := \mathbf{y}'' \cdot \mathbf{y}'' + \lambda\ (\mathbf{y}' \cdot \mathbf{y}'')^2$. The corresponding Euler-Lagrange equations [8] are

$$\begin{aligned} 0 &= -\frac{d}{ds} f_{\mathbf{y}'} + \frac{d^2}{ds^2} f_{\mathbf{y}''} \\ &= \mathbf{y}^{(4)} + \lambda(\mathbf{y}'' \cdot \mathbf{y}'' + \mathbf{y}' \cdot \mathbf{y}^{(3)})\mathbf{y}'' + \lambda(3\mathbf{y}'' \cdot \mathbf{y}^{(3)} + \mathbf{y}' \cdot \mathbf{y}^{(4)})\mathbf{y}'. \end{aligned}$$

A curve that satisfies the above Euler-Lagrange equations, the proper boundary conditions, and the constraint $\int_0^1 (\mathbf{y}' \cdot \mathbf{y}'')^2 ds = 0$ is a critical point of the energy functional. We note that the Lagrangian multiplier in the unconstrained length problem is a cost induced from reducing the curvature expression into $\|\mathbf{y}''(s)\|$.

2.2 The constrained length problem

Next, we consider the case when the total length L of a curve $\mathbf{y}$ is fixed, that is

$$\int_0^1 \|\mathbf{y}'\|\ ds = L. \tag{4}$$

Again, for $J(\mathbf{y})$ in equation (2) to hold, we must impose a fixed speed parametrization. Imposing the constraint

$$\int_0^1 (\mathbf{y}' \cdot \mathbf{y}' - L^2)^2 ds = 0$$

ensures a constant speed parametrization $\|\mathbf{y}'(s)\| = L$, which implicitly imposes the length constraint. Applying the Lagrangian multiplier method, we obtain the constrained energy minimization problem:

$$\text{Minimize } J_\lambda(\mathbf{y}(s)) = \int_0^1 \left\{\mathbf{y}'' \cdot \mathbf{y}'' + \lambda\ (\mathbf{y}' \cdot \mathbf{y}' - L^2)^2\right\} ds. \tag{5}$$

Let $f(\mathbf{y}', \mathbf{y}'') := \mathbf{y}'' \cdot \mathbf{y}'' + \lambda(\mathbf{y}' \cdot \mathbf{y}' - L^2)^2$. The corresponding Euler-Lagrange equations are [8]

$$\begin{aligned} 0 &= -\frac{d}{ds} f_{\mathbf{y}'} + \frac{d^2}{ds^2} f_{\mathbf{y}''\mathbf{y}''} \\ &= \mathbf{y}^{(4)} - 2\lambda(\mathbf{y}' \cdot \mathbf{y}' - L^2)\mathbf{y}'' - 4\lambda(3\mathbf{y}' \cdot \mathbf{y}'')\mathbf{y}'. \end{aligned} \tag{6}$$

A curve that satisfies the Euler-Lagrange equations (6), the length constraint (4), and the proper boundary conditions is a critical point of the functional. In this case, we found a sufficient condition to check if our computed solution of the minimal energy curve is indeed a local minimizer.

Theorem 2.1 *Let $\mathbf{y}_*$ be the solution of (6) when $\lambda = \lambda_*$. Then a sufficient condition for $\mathbf{y}_* = (y_1, y_2, y_3)$ being a minimizer of (2) with length constraint (4) is*

1. $\pi^2 + 2\lambda(\mathbf{y}_*' \cdot \mathbf{y}_*' - L^2) > 0$, *if* $\lambda_* > 0$
2. $\pi^2 + 8\lambda c^* + 2\lambda(\mathbf{y}_*' \cdot \mathbf{y}_*' - L^2) > 0$, *if* $\lambda_* < 0$

where $c^* = \max\{(1 + c_1 + \frac{1}{c_3})(y_1')^2, (1 + \frac{1}{c_1} + c_2)(y_2')^2, (1 + \frac{1}{c_2} + c_3)(y_3')^2\}, c_i > 0, i = 1, 2, 3.$

The proof of the sufficient condition is in Appendix 5.1.

2.3 A simpler parameterization

Above, we described the conduit centerline by $\mathbf{y}(s) = (x(s), y(s), z(s))$, $s \in [0, 1]$. If the conduit centerline can be parameterized as a function of one of its components, this yields the advantage of reducing the number of Euler-Lagrange differential equations by one, and no Lagrangian multiplier is required for the unconstrained length problem. However, many curves cannot be represented in this form, and the fully parameterized approach is more robust (e.g., see Figure 2).

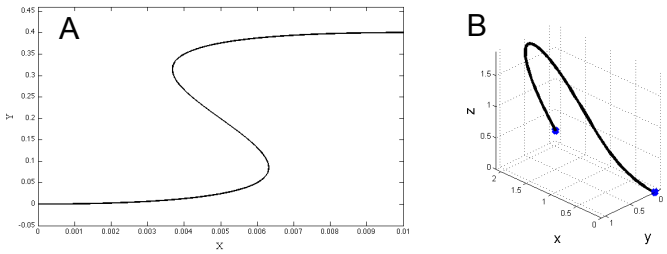

Figure 2: *Examples of minimal energy curves. (a) This curve cannot be represented by* $(x, y(x))$*. (b) This curve cannot be represented by* $(x(z), y(z), z)$*.*

Below, we write the reduced Euler-Lagrange equations under the simpler parameterization $\mathbf{y}(z) = (x(z), y(z), z)$, $z \in [a, b]$. We are given the two endpoints of the curve (x_a, y_a, a) and (x_b, y_b, b) as well as the slopes. Under this formulation, the differential arc length is $ds = \sqrt{1 + x'^2 + y'^2}dz$, and the curvature becomes $\kappa = \frac{\sqrt{x''^2 + y''^2 + (x'y'' - x''y')^2}}{(1 + x'^2 + y'^2)^{\frac{3}{2}}}$.

2.3.1 The free length problem

The energy functional, which is the integral of curvature squared, is

$$J(x, y) = \int_a^b \frac{x''^2 + y''^2 + (x'y'' - x''y')^2}{(1 + x'^2 + y'^2)^{\frac{5}{2}}} \, dz. \tag{7}$$

The corresponding Euler-Lagrange equations for minimizing J can be written in a linear (with respect to the fourth derivative) form

$$\begin{cases} A_1 \cdot x^{(4)} + B_1 \cdot y^{(4)} + R_1 = 0 \\ A_2 \cdot x^{(4)} + B_2 \cdot y^{(4)} + R_2 = 0, \end{cases} \tag{8}$$

where the forms of A_i, B_i, and R_i are given in Appendix 5.2. This linearity in the fourth derivative is amenable for solving the system of fourth order ODEs by transforming them into a system of

first order ODEs. The boundary conditions are the fixed ends $x(a) = x_a$, $y(a) = y_a$, $x(b) = x_b$, and $y(b) = y_b$ and specified slopes $x'(a) = v_{xa}$, $y'(a) = v_{ya}$, $x'(b) = v_{xb}$, and $y'(b) = v_{yb}$.

2.3.2 The constrained length problem

The length constraint is

$$\int_a^b \sqrt{1 + (x')^2 + (y')^2}\, dz = L, \tag{9}$$

and we apply the method of Lagrangian multipliers and introduce the scalar λ to modify the above minimization problem to:

$$\text{Minimize } \tilde{J}_\lambda(x, y) = \int_a^b \frac{x''^2 + y''^2 + (x'y'' - x''y')^2}{(1 + x'^2 + y'^2)^{\frac{5}{2}}}\, dz + \lambda \left(\int_a^b \sqrt{1 + (x')^2 + (y')^2}\, dz - L \right). \tag{10}$$

The resulting Euler-Lagrange equations are

$$\begin{cases} \dfrac{A_1 \cdot x^{(4)} + B_1 \cdot y^{(4)} + R_1}{\left(1 + (x')^2 + (y')^2\right)^3} - \lambda(x'' + x''(y')^2) = 0 \\ \\ \dfrac{A_2 \cdot x^{(4)} + B_2 \cdot y^{(4)} + R_2}{\left(1 + (x')^2 + (y')^2\right)^3} - \lambda(y'' + y''(x')^2) = 0, \end{cases} \tag{11}$$

where A_i, B_i, and R_i are the same as in (8) and are given in Appendix 5.2. Again, the above differential equation is linear in the fourth order derivative and is subject to the same boundary conditions as above.

3 Numerical Method and Simulations

To approximate the solution $\mathbf{y}(s) = (x(s), y(s), z(s))$ to the resulting Euler-Lagrange equations, which form a boundary value problem with a system of fourth order ordinary differential equations, we use the method of collocation. We find that the built-in MATLAB ODE solver `bvp4c`, which uses the three-stage Lobatto IIIa formula [7], is incapable of converging to the solution for many circumstances, while the collocation method is successful in every circumstance we encountered. The essence of the collocation method is to approximate $x(s)$, $y(s)$, and $z(s)$ by a linear combination of a finite number of basis functions and force the approximation to agree exactly with the ordinary differential equations and boundary conditions at an appropriate number of points in the domain (the collocation points). The collocation method is the method of weighted residuals when delta functions at the collocation points are chosen as weight functions [6] and is a well-known method for solving boundary value problems [2]. We define the approximation to the solution $\mathbf{y}(s)$ as:

$$\hat{x}(s) := \sum_{i=-2}^{N+2} \alpha_i \phi_i(s), \;\; \hat{y}(s) := \sum_{i=-2}^{N+2} \beta_i \phi_i(s), \;\; \hat{z}(s) := \sum_{i=-2}^{N+2} \gamma_i \phi_i(s). \tag{12}$$

Here, we choose the set of piecewise, fifth order polynomials as our approximating space and impose C^4 continuity. A polynomial of at least degree 5 is needed in order to represent the spatially varying fourth derivative in the Euler-Lagrange equations. A suitable choice for the basis functions ϕ_i for the space of fifth order, piecewise polynomials with C^4 continuity are the quintic B-spline polynomials [3] ('B' is for 'basis'), one of which is plotted in Figure 3. The definitions of the basis functions in the approximations in (12) correspond to $N+1$ knot points in the domain $[0, 1]$, which we discretize with uniform spacing h and define $s_i := ih$. The forms of the quintic B-spline polynomials can be found in [9, 10], and we use the forms in [9] given in Appendix 5.3.

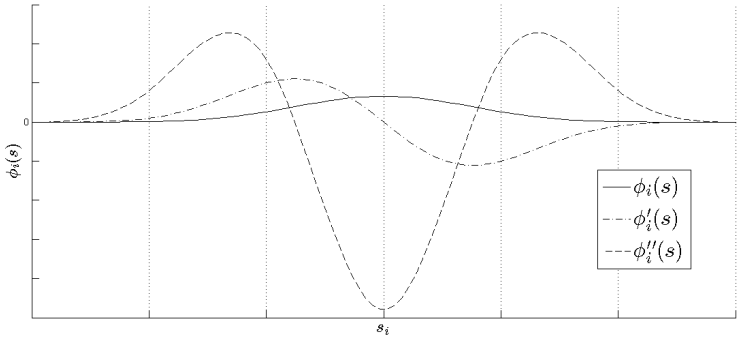

Figure 3: *A quintic B-spline polynomial and its first and second derivatives. The knot points in the s-domain are indicated by vertical dotted lines. The peak of the function $\phi_i(s)$ is at s_i. The spline $\phi_i(s)$ is zero outside of this figure.*

We force the approximations $\hat{x}(s)$, $\hat{y}(s)$, and $\hat{z}(s)$ to agree with the ODEs and boundary conditions at the collocation points, which we choose to coincide with the knot points used to define the B-splines. This results in a system of nonlinear equations to solve for $\{\alpha_i, \beta_i, \gamma_i\}$ that approximates the solution via the expressions in (12). Because of the local life of the B-splines, inside of each element (s_i, s_{i+1}), a weighted sum with respect to α_i (β_i, γ_i) of six different basis functions represents the value of $x(s)$ ($y(s)$, $z(s)$), resulting in a manageable, banded Jacobian matrix [4]. Since each basis function $\phi_i(s)$ lives only on $[s_{i-3}, s_{i+3}]$ and is zero at the end points s_{i-3} and s_{i+3} for continuity, the collocation equation at a point s_i involves only $\{\alpha_k, \beta_k, \gamma_k\}_{k=i-2,i-1,i,i+1,i+2}$.

In problems with a Lagrangian multiplier λ, we iterate on λ and solve the Euler-Lagrange equations until the constraint is satisfied. For example, consider the constrained length problem in Section 2.3.2 and suppose $(x_\lambda(z), y_\lambda(z))$ is the solution of equations (11) with proper boundary conditions for a fixed λ. Define

$$\Upsilon(\cdot): \quad \lambda \mapsto \int_a^b \sqrt{1 + (x_\lambda')^2 + (y_\lambda')^2}\, dz.$$

If there exists a λ^* such that $\Upsilon(\lambda^*) = L$, then $(x_{\lambda^*}, y_{\lambda^*})$ is a (stationary) solution of the constrained length problem. We use an optimization routine in MATLAB `fminsearch` to iterate on λ until

the constraint is satisfied to find an approximation to y_{λ^*} for problems involving a Lagrangian multiplier.

Example 1 We consider a constrained length problem ($L = 1.85$) in three dimensional space with fixed ends at $(0, 0, 0)$ and $(0, 1, 1)$. In representing the curve as $\mathbf{y}(z) = (x(z), y(z), z)$ and defining the following slopes

$$x'(0) = y'(0) = 1, , x'(1) = -1, y(1) = 1, y'(1) = -1, \tag{13}$$

this will intuitively generate a curve that can be parameterized in z. Numerically solving equations (11) and iterating on λ until the length constraint is satisfied results in the curve in Figure 4, which satisfies the proper length constraint $L = 1.85$.

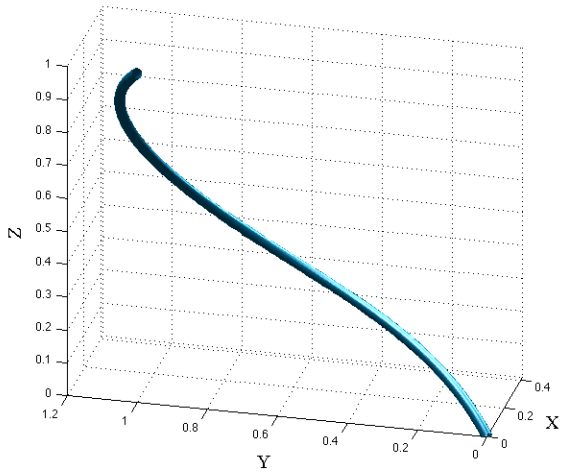

Figure 4: *Example 1*

Example 2 Here, we compute the shape of a conduit of fixed length ($L = 0.54$ units) with fixed ends at $(0, 0, 0)$ and $(0, 0, 0.2)$ and consider when the slope of the fittings changes with time. The time scale of the fitting slope changes must be slow in comparison to the time for the hose to achieve its new equilibrium for our approach to be valid. The video found in Additional File 1 shows the evolution of the shape of the conduit and is an example of how a conduit attached to a moving part might be simulated. The boundary condition $\frac{dx}{dy}$ varies from -1.0 to 1.0.

Example 3 We consider a scenario where two ends of the conduit are fixed at $\mathbf{y}(0) = (0, 0, 0)$ and $\mathbf{y}(1) = (1, 1, 1)$ with corresponding tangent vectors $\mathbf{y}'(0) = (0, 0, 1)$ and $\mathbf{y}'(1) = (0, 0, -1)$. Physically, these tangent vectors correspond to two vertically oriented attachments. We constrain the length of the curve and compute the shape with different lengths varying from $L = 2$ units to $L = 10$ units. This corresponds to a situation where a tube is attached vertically to the top of, say, a box, and is fed vertically through the floor (hence increasing the length). The video in Additional File 2 shows the evolution of the shape as the length changes. Note that the curve in the video is not a function of z and equations (6) are used.

4 Discussion and Conclusions

This paper serves as a reference for the Euler-Lagrange equations for minimizing the elastic energy functional of a bent conduit. We are operating under the assumption that gravity, torsional effects, and shape memory play negligible roles in determining the shape so that the energy functional is proportional to the integral of the square curvature. For each simulation, we considered boundary conditions corresponding to the physical situation that the hose is attached via fittings at specified slopes. Furthermore, we considered both the cases where the length of the conduit is free and where the length is constrained. The manufacturer of the conduit might have only certain lengths, motivating the fixed length constraint problem. The unconstrained length energy minimization is for when the engineer has control over the length and is concerned with minimizing the stress imposed on a bent conduit. However, in most circumstances one will want to keep the length at a practical minimum in order to reduce weight used in construction of the aircraft.

The fully parametric representation $\mathbf{y}(s) = (x(s), y(s), z(s))$ of the curve that models the centerline of the conduit is the most robust representation. However, in reducing the expression for the square of the curvature into the simple expression $\mathbf{y}'' \cdot \mathbf{y}''$ via imposing a constant speed parameterization, a Lagrangian multiplier is needed– even in the unconstrained length case (Section 2.1). This requires iterations on the Lagrangian multiplier λ and more computation time in comparison to the unconstrained length case when the curve can be parameterized by one of its components $\mathbf{y}(z) = (x(z), y(z), z)$ (Section 2.3.1). Another advantage of when a curve can be parameterized by one its components (Section 2.3) is that the number of Euler-Lagrange differential equations is reduced by one. In large-scale modeling with multiple conduits, the fully parametric representation is the practical approach, since the issue where the curve cannot be parameterized by one of its components will likely arise.

For future work, several interacting conduits can be considered where the attachments are moving, such as conduits during landing gear retraction. Example 2 illustrates how a conduit attached to a moving part might be simulated. One might seek a design such that the hoses do not interact. This involves writing robust software that computes the equilibrium shapes of the hoses as the boundary conditions change with time. If a more accurate description is required for certain applications, gravity, torsion, and shape memory might be considered. For these considerations, however, one needs knowledge of the physical properties of the conduits, such as Young's modulus, in order to compare the contribution of each effect on the energy. The simulation of the equilibrium shape of a conduit in this work is only one step towards a large-scale simulation of the myriad of conduits on an aircraft, where several hoses interact with each other and the boundary conditions are changing as parts move.

Acknowledgements

Thanks to Tom Grandine of The Boeing Company for his support in mentoring our team and guiding this project. Thanks to the Institute for Mathematics and its Applications (IMA) and Fadil Santosa at the University of Minnesota for the Math in Industry workshop, where the bulk of this work was done. Thanks to the IMA and the Pacific Institute for Mathematical Sciences (PIMS) for financial support. We thank the anonymous reviewers and MICS editor Hilary Ockendon for helpful comments.

5 Appendix

5.1 A: Deriving a sufficiency condition

Here, we prove the sufficiency condition in Theorem 2.1 for a solution $\mathbf{y}$ of the Euler-Lagrange equation (6) for the constrained length parametric representation of a conduit.

Lemma 5.1 (Wirtinger's inequality) *Suppose v is a C^1 function such that $v(0) = v(a) = 0$. Then*

$$\int_0^a |v|^2 \leq \left(\frac{a}{\pi}\right)^2 \int_0^a |v'|^2.$$

1. Since $\lambda > 0$, we obtain

$$\begin{aligned}
\frac{d^2}{d\epsilon^2} J(\mathbf{y}+\epsilon\mathbf{v})|_{\epsilon=0} &= \int_0^1 2(\mathbf{v}''\cdot\mathbf{v}'') + 16\lambda(\mathbf{y}'\cdot\mathbf{v}')^2 + 4\lambda(\mathbf{v}'\cdot\mathbf{v}')(\mathbf{y}'\cdot\mathbf{y}' - L^2)\, ds \\
&\geq \int_0^1 2(\mathbf{v}''\cdot\mathbf{v}'') + 4\lambda(\mathbf{v}'\cdot\mathbf{v}')(\mathbf{y}'\cdot\mathbf{y}' - L^2)\, ds \\
&\geq \int_0^1 2\pi^2(\mathbf{v}'\cdot\mathbf{v}') + 4\lambda(\mathbf{v}'\cdot\mathbf{v}')(\mathbf{y}'\cdot\mathbf{y}' - L^2)\, ds \\
&= \int_0^1 2(\mathbf{v}'\cdot\mathbf{v}')[\pi^2 + 2\lambda(\mathbf{y}'\cdot\mathbf{y}' - L^2)]\, ds, \\
&> 0,
\end{aligned}$$

where we apply Lemma 5.1 to the second inequality.

2. Since $\lambda < 0$, we obtain

$$\begin{aligned}
\frac{d^2}{d\epsilon^2} J(\mathbf{y}+\epsilon\mathbf{v})|_{\epsilon=0} &= \int_0^1 2(\mathbf{v}''\cdot\mathbf{v}'') + 16\lambda(\mathbf{y}'\cdot\mathbf{v}')^2 + 4\lambda(\mathbf{v}'\cdot\mathbf{v}')(\mathbf{y}'\cdot\mathbf{y}' - L^2)\, ds \\
&\geq \int_0^1 2(\mathbf{v}''\cdot\mathbf{v}'') + 16\lambda c^*(\mathbf{v}'\cdot\mathbf{v}') + 4\lambda(\mathbf{v}'\cdot\mathbf{v}')(\mathbf{y}'\cdot\mathbf{y}' - L^2)\, ds \\
&\geq \int_0^1 2\pi^2(\mathbf{v}'\cdot\mathbf{v}') + 16\lambda c^*(\mathbf{v}'\cdot\mathbf{v}') + 4\lambda(\mathbf{v}'\cdot\mathbf{v}')(\mathbf{y}'\cdot\mathbf{y}' - L^2)\, ds \\
&= \int_0^1 2(\mathbf{v}'\cdot\mathbf{v}')[\pi^2 + 8\lambda c^* + 2\lambda(\mathbf{v}'\cdot\mathbf{v}')(\mathbf{y}'\cdot\mathbf{y}' - L^2)]\, ds \\
&> 0,
\end{aligned}$$

where for the first inequality, we use the fact that

$$(\mathbf{y}' \cdot \mathbf{v}')^2 \leq c^*(\mathbf{v}' \cdot \mathbf{v}'). \tag{14}$$

And we apply Lemma 5.1 for the second inequality. The proof of (14) is the following:

$$\begin{aligned}
(\mathbf{y}' \cdot \mathbf{v}')^2 &= (y_1'v_1' + y_2'v_2' + y_3'v_3')^2 \\
&= (y_1'v_1')^2 + (y_2'v_2')^2 + (y_3'v_3')^2 + 2y_1'v_1'y_2'v_2' + 2y_2'v_2'y_3'v_3' + 2y_3'v_3'y_1'v_1' \\
&\leq (y_1'v_1')^2 + (y_2'v_2')^2 + (y_3'v_3')^2 + c_1(y_1'v_1')^2 \\
&\quad + \frac{1}{c_1}(y_2'v_2')^2 + c_2(y_2'v_2')^2 + \frac{1}{c_2}(y_3'v_3')^2 + c_3(y_3'v_3')^2 + \frac{1}{c_3}(y_1'v_1')^2 \\
&= (1 + c_1 + \frac{1}{c_3})(y_1'v_1')^2 + (1 + c_2 + \frac{1}{c_1})(y_2'v_2')^2 + (1 + c_3 + \frac{1}{c_2})(y_3'v_3')^2 \\
&\leq c^*((v_1')^2 + (v_2')^2 + (v_3')^2) \\
&= c^*(\mathbf{v}' \cdot \mathbf{v}').
\end{aligned}$$

5.2 B: Defining the condensed forms of the Euler-Lagrange equation (8)

These are the forms of the shorthand notation used in writing the Euler-Lagrange equation (8):

$$\begin{aligned}
A_1 &:= 2(1 + x'^2 + y'^2)^2(1 + y'^2), \\
B_1 &:= -2x'y'(1 + x'^2 + y'^2)^2, \\
R_1 &:= (1 + x'^2 + y'^2)\big\{2(1 + x'^2 + y'^2)(2y^{(3)}(x''y' - x'y'') + 3y''(x^{(3)}y' \\
&\quad + x'y^{(3)}) + y'(x^{(3)}y'' - x''y^{(3)})) - 2(x'x'' + y'y'')(3x^{(3)} + y''(x''y' \\
&\quad - x'y'') + 3y'(x^{(3)}y' - x'y^{(3)})) - 10(x'x^{(3)} + x''^2 + y'y^{(3)} + y''^2) \\
&\quad \cdot(x'' + y'(x''y' - x'y'')) + 5\big[x''^3 + x''y''^2 + x''(x'y'' - x''y')^2 \\
&\quad + 2x'\big(x''x^{(3)} + y''y^{(3)} - (x'y'' - x''y')(x^{(3)}y' - x'y^{(3)})\big)\big]\big\} \\
&\quad - 7(x'x'' + y'y'')\big[2(1 + x'^2 + y'^2)\big(x^{(3)} + 2y''(x''y' - x'y'') \\
&\quad + y'(x^{(3)}y' - x'y^{(3)})\big) - 10(x'x'' + y'y'')\big(x'' + y'(x''y - x'y'')\big) \\
&\quad + 5x'\big(x''^2 + y''^2 + (x'y'' - x''y')^2\big)\big],
\end{aligned}$$

$$
\begin{aligned}
A_2 &:= -2x'y'(1+x'^2+y'^2)^2,\\
B_2 &:= 2(1+x'^2+y'^2)^2(1+x'^2),\\
R_2 &:= (1+x'^2+y'^2)\big\{2(1+x'^2+y'^2)(-2x^{(3)}(x''y'-x'y'')+3x''(x^{(3)}y'\\
&\quad +x'y^{(3)})-x'(x^{(3)}y''-x''y^{(3)}))-2(x'x''+y'y'')(3y^{(3)}-x''(x''y'\\
&\quad -x'y'')-3x'(x^{(3)}y'-x'y^{(3)}))-10(x'x^{(3)}+x''^2+y'y^{(3)}+y''^2)\\
&\quad \cdot(y''-x'(x''y'-x'y''))+5\big[y''^3+y''x''^2+y''(x'y''-x''y')^2\\
&\quad +2y'\big(x''x^{(3)}+y''y^{(3)}-(x'y''-x''y')(x^{(3)}y'-x'y^{(3)})\big)\big]\big\}\\
&\quad -7(x'x''+y'y'')\big[2(1+x'^2+y'^2)\big(y^{(3)}-2x''(x''y'-x'y'')\\
&\quad -x'(x^{(3)}y'-x'y^{(3)})\big)-10(x'x''+y'y'')\big(y''-x'(x''y-x'y'')\big)\\
&\quad +5y'\big(x''^2+y''^2+(x'y''-x''y')^2\big)\big].
\end{aligned}
$$

5.3 C: Quintic B-spline basis functions for collocation method

The forms of the quintic B-spline polynomials can be found in [9, 10], and we use the forms in [9] here:

$$
\phi_i(s)=\frac{1}{h^5}\begin{cases}
(s-s_{i-3})^5, & s\in[s_{i-3},s_{i-2})\\
(s-s_{i-3})^5-6(s-s_{i-2})^5, & s\in[s_{i-2},s_{i-1})\\
(s-s_{i-3})^5-6(s-s_{i-2})^5+15(s-s_{i-1})^5, & s\in[s_{i-1},s_i)\\
(s_{i+3}-s)^5-6(s_{i+2}-s)^5+15(s_{i+1}-x)^5, & s\in[s_i,s_{i+1})\\
(s_{i+3}-s)^5-6(s_{i+2}-s)^5, & s\in[s_{i+1},s_{i+2})\\
(s_{i+3}-s)^5, & s\in[s_{i+2},s_{i+3})\\
0 & \text{otherwise}
\end{cases}
$$

The quintic B-spline $\phi_i(s)$ has the following properties:

- ϕ_i is nonzero only inside the interval (s_{i-3}, s_{i+3}).
- ϕ_i is continuous and so are its first, second, third, and fourth derivatives.

Additional Files

Additional file 1 — Video of changing boundary conditions

Here, the shape of a conduit of fixed length is computed while changing the specified slope at which the ends are attached. The fixed length of the conduit is 0.54 units with its two ends fixed at $(0,0,0)$ and $(0,0,0.2)$. In the video, we vary the boundary condition $\frac{dx}{dy}$ from -1.0 to 1.0.

Additional file 2 — Video of conduit as length changes with time

Imagine a conduit being fed through the bottom of the floor to a vertical attachment above. This shows the evolution of the shape of the conduit as the length changes.

References

[1] J. Arroyo, O. Garay, and J. Mencia, *Closed generalized elastic curves in $S^2(1)$*, Journal of Geometry and Physics **48** (2003), 339–353. 2

[2] U. Ascher, R. Mattheij, and R. Russell, *Numerical solution of boundary value problems for ordinary differential equations*, SIAM Classics (1995). 6

[3] C. De Boor, *A practical guide to splines*, Applied Mathematical Sciences **27** (1978), Springer-Verlag, New York. 7

[4] I. Dag, B. Saka, and A. Boz, *Quintic B-Spline Galerkin Method for Numerical Solutions of the Burgers' Equation*, Applied Mathematics and Computation **166** (2005), no. 3, 506–522. 7

[5] L. Evans, *Partial differential equations*, American Mathematical Society (1998).

[6] B. Finlayson and L. Scriven, *The Method of Weighted Residuals- A review*, Applied Mechanics Reviews **19** (1966), 735–748. 6

[7] M. W. Reichelt L. F. Shampine and J. Kierzenka, *Solving boundary value problems for ordinary differential equations in MATLAB with* `bvp4c`. 6

[8] C. Lanczos, *The variational principles of mechanics*, Dover Publications (1986). 3, 4

[9] R. Mittala and G. Arora, *Quintic B-spline collocation method for numerical solution of the Kurmoto-Sivashinsky equation*, Communications in Nonlinear Science Numerical Simulation **15** (2010), 2798–2808. 7, 12

[10] B. Saka, Y. Dag, and D. Irk, *Quintic B-Spline Collocation Method for Numerical Solution of the RLW Equation*, Anziam J **49** (2008), 389–410. 7, 12